

Cover Page



Universiteit Leiden

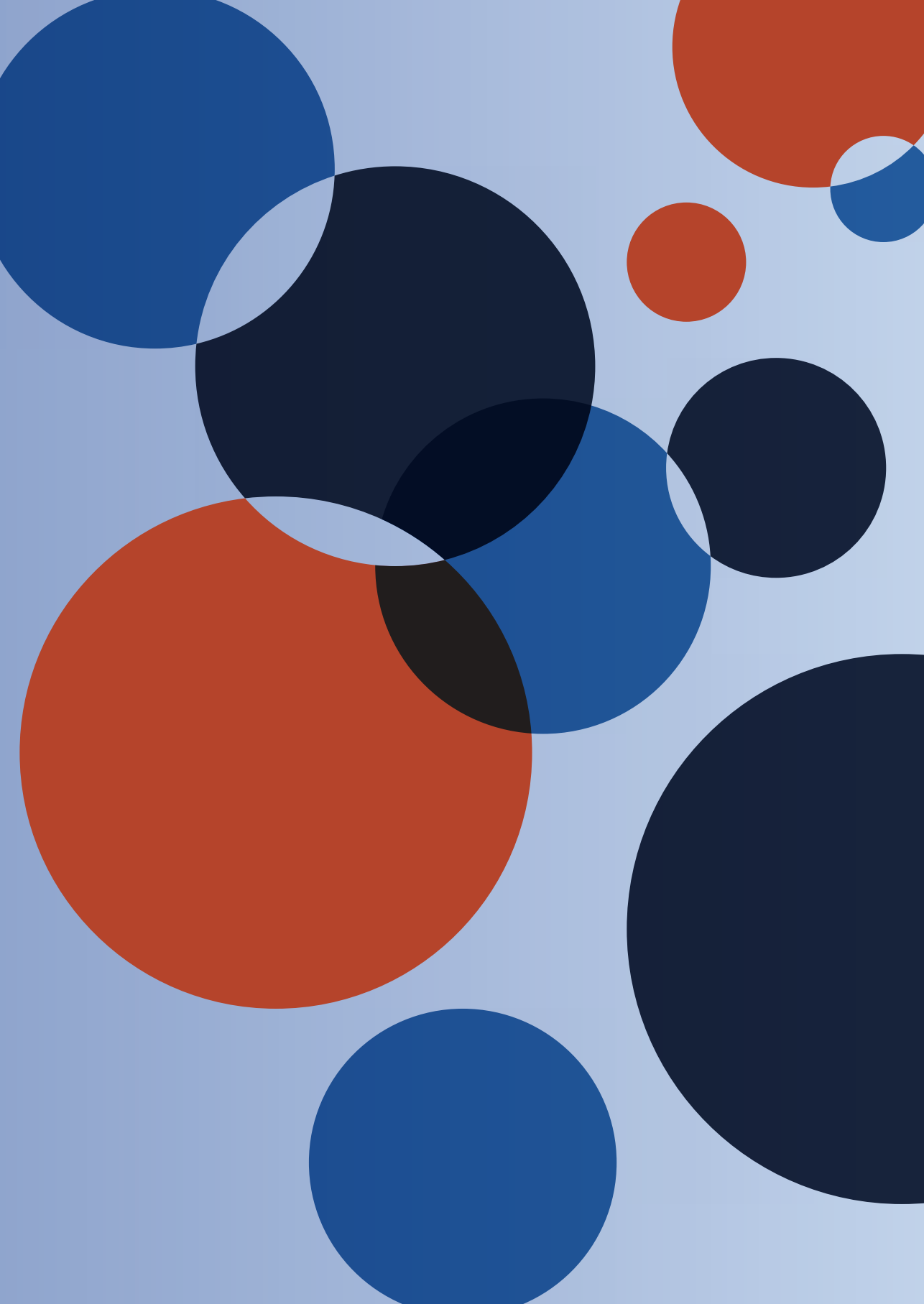


The handle <http://hdl.handle.net/1887/138822> holds various files of this Leiden University dissertation.

Author: Tilburg, J.

Title: The role of solute carrier family 44 member 2 in the pathophysiology of venous thrombosis

Issue date: 2021-01-07



SLC44A2/HNA-3A IS INVOLVED IN NEUTROPHIL ADHESION AND ACTIVATION TO VON WILLEBRAND FACTOR IN HUMANS AND MICE

Gaïa Zirka, Julia Tilburg, Philippe Robert, Chrissta X. Maracle, Bart J.M. van Vlijmen,
Paulette Legendre, Marie-Christine Alessi, Peter J. Lenting,
Pierre-Emmanuel Morange and Grace M. Thomas

Manuscript under revision.

5

Abstract

Background

Genome wide association studies linked expression of the HNA-3a (human neutrophil antigen-3a) epitope on the solute carrier family 44 member 2 (SLC44A2) protein with venous thrombosis (VT) in humans. Expression of the HNA-3b is associated with a 30% decreased risk of VT. SLC44A2 is a ubiquitous transmembrane protein identified as a receptor for Von Willebrand factor (VWF).

Aims

To explain the link between SLC44A2 and VT we wanted to determine how SLC44A2 expressing either HNA-3a or HNA-3b on neutrophils could modulate their adhesion and activation on VWF under flow.

Methods

Transfected HEK293T cells or neutrophils homozygous for the HNA-3a- or the HNA-3b-coding allele purified from healthy donors were perfused in flow chambers at venous shear rates (100s^{-1}). Different matrices including VWF and blocking antibodies were tested. Neutrophil activation by lipopolysaccharide (LPS) was evaluated at various cell concentrations in different flow conditions. Neutrophil mobilization was also measured by intravital microscopy in venules from SLC44A2 deficient mice and wildtype controls after histamine-induced endothelial degranulation and anti-Ly6G staining.

Results

HNA-3a expression was required for SLC44A2-mediated neutrophil adhesion to VWF at 100s^{-1} . This adhesion could occur independently of beta-2 integrin engagement. We observed that adhesion of HNA-3a-expressing neutrophils was enhanced when they were preactivated with LPS. Moreover, specific shear conditions could act as a “second hit” on those, increasing their activation and inducing the formation of neutrophil extracellular traps. *In vivo*, mice lacking SLC44A2 showed a massive reduction in neutrophil recruitment in inflamed mesenteric venules.

Conclusions

Our results show that SLC44A2/HNA-3a is important in the adhesion and activation process of neutrophils in veins under inflammation and when submitted to specific shears conditions. Neutrophils expressing SLC44A2/HNA-3b not being associated with these observations, these results could thus explain the association between the HNA-3b epitope and the reduced risk for VT in humans.

Introduction

Venous thromboembolic (VT) disease is the third cause of cardiovascular death after myocardial infarction and stroke in industrialized countries. It includes deep vein thrombosis and pulmonary embolisms. Using genome wide association study (GWAS) approaches and transgenic mice our team and others have contributed to the identification of *SLC44A2* as a new gene involved with VT both in humans (1, 2) and in mice (3). In-depth analysis of the *SLC44A2* locus identified rs2288904 (461G>A; Arg154Gln) as the functional variant responsible for the association with VT. This polymorphism corresponds to the expression of the HNA-3a (human neutrophil antigen-3a, Arg154) or HNA-3b antigen (Gln154) expression by the *SLC44A2* (4-6). Homozygosity for the HNA-3b-coding allele is associated with a decreased risk of VT of ~30% (2).

SLC44A2 is an ubiquitous transmembrane protein of 70-95kDa (7). It is a choline carrier system proposed to supply choline for the cell membrane phospholipids (8). However, because of alternative splicing, *SLC44A2* from blood circulating cells is not able to transport choline, thus suggesting another function in these cells (9). *SLC44A2* has been identified in 2015 as a new receptor for Von Willebrand factor (VWF) (10). VT is a multifactorial disease which mechanisms still remained to be fully uncovered. Until recently, pathophysiology of VT was only based on the original cascade model of coagulation. Accumulating data has highlighted mechanisms independent of coagulation cascade on clot formation. These last few years animal studies have shown that neutrophils (11, 12) VWF (13) play a crucial role in the VT process. As the *SLC44A2* gene does not belong to the coagulation/fibrinolytic cascades, dissecting the mechanisms involved in its relation with VT is a powerful strategy to generate new biological knowledge of the underlying pathophysiology and ultimately to develop novel clinical therapies to limit bleeding and prevent recurrent and primary VT. *SLC44A2* has been associated with transfusion acute-lung injury (TRALI) which is the leading cause of transfusion-associated mortality in developed countries (Mair and Eastlund, 2010). The most severe cases of TRALI have been associated with alloantibodies reacting against the HNA-3a epitope exposed by *SLC44A2*, the same antigen associated to VT. We and others have shown that alloantibodies targeting *SLC44A2* can lead to neutrophil activation and formation of Neutrophil extracellular traps (NETs) by primed HNA-3a positive neutrophils (14, 15). Neutrophil recruitment to the endothelium and neutrophil activation/NETosis are key steps in TRALI (14, 16) but also in arterial thrombosis (17) and in VT (11, 18, 19). After adhesion to the activated endothelium, neutrophils initiate and propagate VT by interacting with platelets and by exposure and activation of circulating tissue factor and FXII (18). Importantly, mice with impaired NETosis have a decreased incidence of thrombosis in a model of VT (12), and mice treated with DNase-1 (which degrades DNA and NETs) are protected in this model (11). As in mice with thrombosis, outcome of mice with TRALI could be improved by having them inhale DNase-1 (14). The TRALI model, though being different from VT physiopathology may pave the way to understand why *SLC44A2* plays a role in VT and why the HNA-3b isoform carrier have a decreased risk of VT. We investigated in this

study whether SLC44A2 could act as an adhesion protein allowing neutrophil adhesion to VWF under flow, and whether SLC44A2 could act as a receptor able to activate neutrophils and stimulate extracellular DNA trap formation.

We demonstrated that SLC44A2 is important in the adhesion and activation process of neutrophils under flow when submitted to inflammation and specific shear conditions. The fact that neutrophils expressing SLC44A2/HNA-3b is not associated with these observations, could thus explain the association between the HNA-3b epitope and the reduced risk for VT in humans.

Material and methods

Cell lines and culture conditions

Human embryonic kidney (HEK)-293T cells non transfected or transfected to overexpress SLC44A2/HNA-3a (R154) or SLC44A2/HNA-3b (Q154) fused with a Green fluorescent protein tag (GFP) were generous gifts from Drs. Daniel Bougie and Brian Curtis from the Bloodcenter of Wisconsin (4, 20). Cells were cultured in Dulbecco's Modified Eagle Medium (DMEM, Gibco) supplemented with 10% Fetal bovine serum (FBS, Gibco), 4mM L-Glutamine (Gibco), 100U/ml penicillin, 100µg/ml streptomycin (Gibco), and 50 µg/mL geneticin (Gibco) when a selection antibiotic was needed. Cells were cultured at 37°C in a humidified atmosphere with 5% CO₂. PBS and Versene (0.48 mM, Gibco) were used for cell dissociation. Single-cell suspensions were obtained after passing the cells through a 70µm cell strainer (Falcon). Cell counts and viability were measured by an automated cell counter after trypan blue staining (EVE™, Nanoentek).

Immunofluorescence staining

Transfected HEK-293 cells were seeded on L-poly-lysine- (0.01%, Gibco) coated coverslips in complete medium. 24 hours later, media was changed. Nonspecific interaction sites were blocked with BSA and cells were incubated with 10µg/ml VWF (LFB) or vehicle control for 1h. Cells were then washed with PBS, fixed with 4% PFA, washed, saturated with Tween/BSA and stained for VWF with 5µg/ml of mouse anti-human VWF antibody (house made monoclonal antibody pool). Secondary antibody staining was done with an Alexa 546-goat anti-mouse IgG (0.4mg/ml, Invitrogen). Nuclei were stained with Dapi (1µg/ml) and f-actin was stained with phalloidin (2µg/ml, invitrogen). Coverslips were then mounted on slides with prolong Gold antifade reagent (Molecular probes). Images were acquired with a Nikon Eclipse E600 microscope with PixelLINKCaptureOEM software. VWF fluorescence per cell was then quantified using ImageJ software.

Human neutrophil isolation

After all participants gave written informed consent, neutrophils were isolated from healthy volunteers' blood at the Timone University Hospital (Marseille, France) who declared that they had not received any medication for at least 2 weeks. Sodium citrate was used as

anticoagulant for blood puncture except if otherwise specified. Neutrophils were prepared as previously described (14). The research was approved by the relevant institutional review boards and ethic committees. The investigation conforms to the principles outlined in the Declaration of Helsinki. After isolation, neutrophils were eventually labeled with the dye of use (Calcein AM 4 μ M, cell trace red orange 4 μ M or DiD 2 μ g/ml). When specified, 1mM CaCl₂ and/or blocking antibodies were added to neutrophils before utilization. Concentration was adjusted and only cells at acceptable viability (>75%) were used.

SLC44A2 genotyping

Donors homozygous for the HNA-3a- or HNA-3b-coding allele were identified by SNP genotyping using a taqman 5' exonuclease PCR technology as previously described (21).

Flow chamber assays

Flow chambers μ -slide VI 0.1 ibitreat (Ibidi) were used for cell speed analysis and NETosis experiments, and Vena8 fluoro + microfluidic biochip (Cellix) were used for NETosis experiments. Flow chambers were coated overnight at 4°C with either 70 μ g/ml VWF (Wilfactin, LFB), VWF recombinant A1-Fc domain (10 μ g/ml), fibrinogen (10 μ g/ml), or BSA (10 μ g/ml, Sigma). After one wash with PBS, saturation was done with PBS/BSA 0.1% 1 hour prior to the assay. If applicable, blocking antibodies (10 μ g/ml; VWF-A1 blocking Ab 318 clone, anti CD18 TS1/18 clone or irrelevant IgG1 and IgG2) were incubated in the channels 30 minutes before cell perfusion and perfused concomitantly at 25 μ g/ml for VWF blockade experiments. Continuous flow rate was applied forward using an electrical syringe pump (bioblock scientific) with a 1ml or 5ml syringe (Terumo) connected to the chamber with silicon tubing (Ibidi or Cellix). One chamber was used per condition and the chambers were discarded after each experiment.

Transfected HEK 293 cells (4) or purified neutrophils were labeled 20 minutes under agitation with either Calcein AM (4 μ M, Life Technologies) or DiD dye (2 μ g/ml) for activation experiments. Cells were washed once in PBS. When indicated, neutrophils were incubated with lipopolysaccharide (LPS 5 or 25 μ g/ml) or MnCl₂ (1mM) for 1 hour prior to cell perfusion and cells were eventually incubated 5 min prior to perfusion with calcium (1mM). Extracellular DNA was labeled by addition of Sytox green or Sytox red (1 μ M, Life Technologies) to the neutrophils immediately before perfusion. Cells (1.5.10⁶ cells/ml) were infused in flow chamber at a wall shear rate of 100s⁻¹ (or other if specified) at a controlled temperature of 37°C using a thermoregulated thermostatic chamber (Olympus). Cells were allowed to pass through the channel for 5 minutes before acquisition. Acquisition was done with an inverted microscope (IX71, Olympus) and a LED fluorescence lamp for sample excitation (SPECTRA X light engine, Lumencor) in three different fields (1329.4 μ m wide) during 1 minute at a rate of 20 images/sec. Real-time imaging was performed using a CMOS digital camera (Orca-Flash 4.0 V2 CCD C11440, Hamamatsu).

Flow chamber cell motion analysis

A dedicated program was written in Java (Oracle, USA) as a plug-in for ImageJ (NIH, USA). Cells were detected as bright areas above a chosen threshold over a dark background. Trajectories of individual cells were formed by calculating in a given image the distance between the barycenter of each cell and adding to the forming trajectory the cell of closest barycenter in the next image, while ensuring that cell area would not change above a chosen threshold. Velocities were calculated for each position of each trajectory long the flow axis, as the mean velocity between to positions separated by a user-chosen interval, to form velocity histograms of either individual cells or whole experiment. Cells were categorized in two groups: "adhesion (<math><10\mu\text{m/s}</math>) and "rolling" (200-500 $\mu\text{m/s}</math>) to simplify cell behavior analysis.$

NET generation in vitro

NET generation was done and quantified as previously described (14). VWF was used at a concentration of 10 $\mu\text{g/ml}$. Imaging was done with the microscope set-up used for flow chamber imaging as described above. Tumor necrosis factor- α (TNF α) was used for cell priming because TNF- α is produced by human neutrophils stimulated by LPS (22) and because commonly used for this assay in other studies.

Mice

11 to 12 week old mice were used. Mice deficient for SLC44A2 (C57BL/6J background) and littermate controls (Slc44a2 $+/+$) were used as previously done (3). Experimental animal procedures were approved by local welfare committees in Aix-Marseille University. Experiments were performed blinded for genotype. For mouse rolling assays, at least 2 venules were recorded for 1 minute each.

Model of endothelial degranulation on mouse mesenteric venules

Intraperitoneal (IP) injection of histamine (13nmol/g of mouse) in 200 μl saline or saline alone (control) was injected 30 minutes prior to mouse anesthesia to induce endothelial degranulation. Mice were anesthetized by IP injection of ketamine (100mg/kg) xylazine (20mg/kg). Mice were then infused through the retro-orbital plexus with 2 $\mu\text{g}/50\mu\text{l}$ of anti-Ly6g antibody (1A8 clone, eBioscience). After laparotomy the mesentery bed was carefully exposed and kept warm and moist by superfusion of warm saline ($\sim 37^\circ\text{C}$). Neutrophil rolling was recorded in 3 different venules by intravital microscopy and quantified over a 1minute timeframe.

Statistical analysis

Data represents mean \pm SEM. Adhesion and rolling experiments were analyzed by Mann-Whitney and Kolmogorov-Smirnov tests. Immunofluorescence experiments were analyzed with one-way ANOVA test. Shapiro-Wilk test was used to check normality. For *in vivo* rolling experiments the population was not normally distributed. As a consequence, data were Log transformed and a test for parametric population was applied. Results were considered significant at $p<0.05$.

Results

The SLC44A2/HNA-3a epitope is necessary for cell adhesion to VWF under flow

We used HEK293T cells transfected to express SLC44A2 with either the HNA-3a epitope (Arg154) or the HNA-3b epitope (Gln154). These cells have been already characterized and express similar levels of SLC44A2 ((4), Figure S1). After incubation of these cells in culture with purified VWF, we observed patches for positive VWF staining 2.6 more intense on HEK293T cells expressing SLC44A2/HNA-3a than on those expressing SLC44A2/HNA-3b (Figure 1, HEK293T/HNA-3a+VWF 65.9 ± 4.2 ; HEK293T/HNA-3b 38.1 ± 2.2). Then, we wanted to confirm the ability of these cells to bind VWF in presence of flow. We perfused fluorescent HEK293T transfected cells in flow chambers coated with VWF and submitted to a “postcapillary venule” shear rate of 100s^{-1} . Digital real time imaging at the speed of 1 frame per 50 ms on $1329\ \mu\text{m}$ -wide fields allowed us to digitally extract precise cell speed data from these experiments. We evaluated for each of the 3 different fields the mean velocity of each cell that passed our cut-off parameters. When we plotted the percentage of cells tracked in function of their speed, we observed for both groups a maximum of HEK293T cells passing at around $1400\text{-}1600\ \mu\text{m/s}$ (Figure 2A). Interestingly we detected also some cells interacting strongly with the matrix (speed $<10\ \mu\text{m/s}$) in the HNA-3a-expressing group.

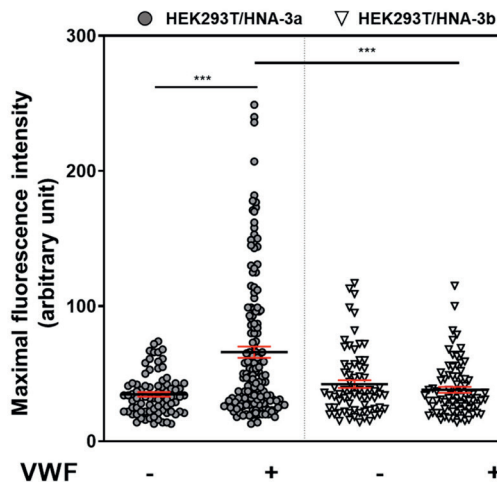


Figure 1. HEK293T/HNA-3a cells bind more to VWF than HEK293T/HNA-3b cells. Quantification of maximal fluorescence intensity recorded per cell and representing anti-VWF staining on transfected HNA-3a- (grey circle) or HNA-3b-expressing HEK293T cells (white triangle) (***) $p < 0.005$.

We compiled the recorded cell velocities in 2 different groups: “adhesion ($<10\ \mu\text{m/s}$) and “Rolling” ($200\text{-}500\ \mu\text{m/s}$). We observed that exposure of HNA-3a by HEK293T cells is associated with cell adhesion to the VWF matrix under flow, whereas HEK293T cells

expressing HNA-3b lose this ability ($1.32 \pm 0.60\%$ against 0% of total tracked cells adhering to the matrix respectively, Figure 2B).

HEK293T cells are not programmed for cell adhesion. We wondered if SLC44A2 could affect VT by modulating neutrophil adhesion to VWF, which is crucial in VT. We genotyped healthy consenting blood donors for the SLC44A2 rs2288904 (R>G154) polymorphism. We purified blood neutrophils only from donors homozygous for the HNA-3a- (R154) or the HNA-3b coding allele (Q154). They were perfused in flow chambers in the same experimental conditions as above. When compared to HEK293T cells, we also observed the majority of the cells going at an approximative speed of $1500\text{-}1600\text{s}^{-1}$, plus others rolling at a speed around 300s^{-1} which is typical for neutrophils (Figure 2C). Here again, we observed that the HNA-3a/3b epitope did not influence “fast rolling” ($200\text{-}500\mu\text{m/s}$) on VWF, whereas HNA-3b-expressing neutrophils showed a significant reduction in cell adhesion on this matrix (Figure 2D). This was not observed in presence of higher shear rates (1000s^{-1} , data not shown) and this adhesion was also inhibited in presence of a specific VWF-A1 domain blocking antibody (Figure 2E).

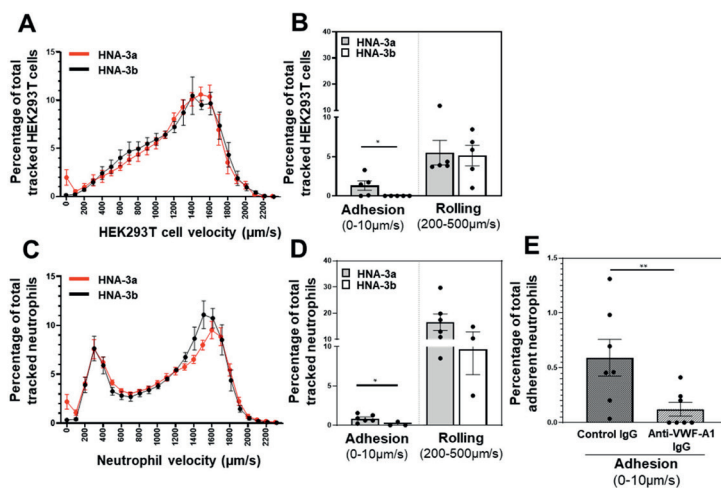


Figure 2. The CTL2/HNA-3a epitope is necessary for cell adhesion to VWF under flow. (A, C) Compiled amount of HEK293T cells (**A**) or neutrophils (**C**) counted in function of their mean velocity ($\mu\text{m/s}$) on coated VWF when submitted to a 100s^{-1} shear rate. Red: HNA-3a-expressing cells; black: HNA-3b expressing cells ($n=5$ donors per genotype, 3 fields per donor). (**B, D**) Graphs depicting the adhesion and rolling profiles of HEK293T cells (**B**) and neutrophils (**D**) perfused on a VWF matrix under flow at a 100s^{-1} shear rate. Perfusion of cells at 100s^{-1} resulted in more adhesion and slow rolling of SLC44A2/HNA-3a expressing HEK293T cells (B, $n=5$ donors per genotype, 3 fields per donor.) and PMN (D, HNA-3a $n=6$ donors p, 3 fields per donor; HNA-3b $n=3$ donors, 3 fields per donor) to human VWF coated channels compared to CTL-2/HNA-3b expressing cells. Adhesion and slow rolling of CTL-2/

HNA-3a expressing PMN (E, n=3) to VWF was blocked by VWF-A1 domain blocking monoclonal antibody. (* $p < 0.05$; ** $p < 0.01$; *** $p < 0.005$)

These data suggest that HNA-3a expression is crucial for HEK293T or neutrophil adhesion to VWF in presence of venule shear rate (100s^{-1}), and confirm the data from another team pointing the involvement of the VWF-A1 domain in VWF/SLC44A2 interactions (10).

Neutrophil adhesion on VWF under flow is amplified after an inflammatory first “hit”

Inflammatory-related disorders often follow the two-hit or multiple-hit hypothesis. HNA-3a-associated VT probably follows this pattern, and this may explain why not all the HNA-3a- positive population will suffer from VT. We thus tested if an inflammatory hit mimicking an infection (LPS), could influence SLC44A2-mediated neutrophil adhesion to VWF. For this, we pre-activated neutrophils with LPS (5 or $25\mu\text{g/ml}$) for 1 hour before perfusion in flow chambers. Our data show that whereas HNA-3b expressing neutrophils do not adhere more to VWF when activated, LPS does increase adhesion of HNA-3a-expressing neutrophil to VWF at 100s^{-1} (Figure 3A). LPS had no effect on “fast rolling” (Figure 3B). The exacerbation of the difference between the HNA-3a and HNA-3b groups in cell adhesion seemed to be present also when lower shear rates were used too (50 and 10s^{-1} , Figure 3C). However, the variations between experiments being higher at lower shear rates, the difficulty to find HNA-3b homozygous donors did not permit us to increase the HNA-3b group size and to conclude for these lower shear rates.

We also observed in the LPS experiment from Figure 3 that the control groups of non-stimulated cells showed higher adhesion rate when compared to the Figure 2 experiments. For LPS experiments, cells received some calcium prior to stimulation in order to replenish their Ca^{2+} intracellular stocks. It is indeed possible that SLC44A2/VWF engagement induces cell and integrin activation that will in return permit the adhesion of neutrophils to VWF under flow.

The fact that the SLC44A2/VWF interaction is followed by the formation of a trimolecular complex composed by SLC44A2, VWF and the $\alpha_{\text{M}}\beta_2$ (Mac-1) integrin (10) supports this hypothesis with the possible existence of a subsequent “outside-in” signaling. Because β_2 integrins are the major integrins involved in neutrophil adhesion, we treated HNA-3a or HNA-3b-expressing neutrophils with either a specific β_2 - (CD18-) blocking antibody or an irrelevant antibody. We then looked at neutrophil adhesion and rolling on VWF at 100s^{-1} (Figure 3D and E). Beta-2 integrin blockade did not abolish neutrophil adhesion to VWF under flow, showing that SLC44A2/HNA-3a mediated neutrophil adhesion to VWF is at least partly beta-2 integrin independent.

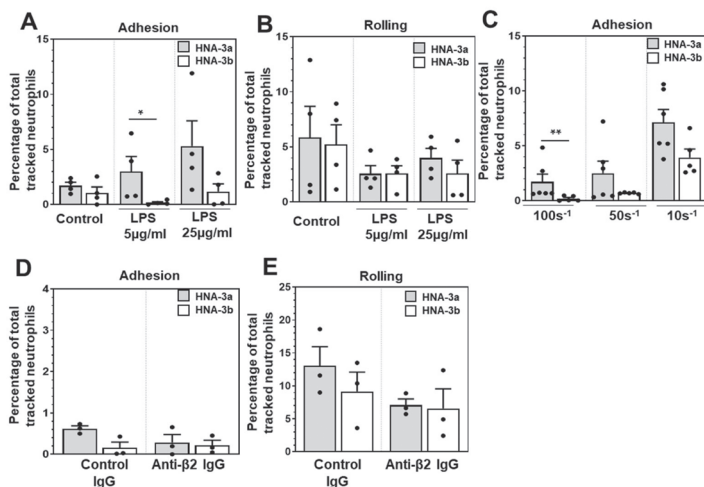


Figure 3. Adhesion of HNA-3a-expressing neutrophils to VWF is amplified by LPS and does not require beta 2 integrins. (A, B) Percentage of total tracked neutrophils qualified as adherent (A) and in “fast rolling” (B) when perfused at 100s⁻¹ on immobilized VWF after LPS treatment (5 µg/ml or 25µg/ml) prior to perfusion (n=4 donors per genotype, 3 fields per donor). (C) Percentage of total tracked neutrophils qualified as adherent or in “slow rolling” when perfused at 100s⁻¹, 50 s⁻¹ and 10s⁻¹ on immobilized VWF (HNA-3a n=5 donors p, 3 fields per donor; HNA-3b n=4 donors, 3 fields per donor). (D, E) Percentage of total tracked neutrophils qualified as adherent (D) and in “fast rolling” (E) when perfused at 100s⁻¹ on immobilized VWF after treatment with a β2 integrin blocking IgG, or a control irrelevant IgG (n=3 donors per genotype, 3 fields per donor). (* p<0.05; ** p<0.01).

SLC44A2/HNA-3a can mediate DNA extracellular trap formation from neutrophils flowing on VWF

The enhanced neutrophil adhesion observed for the SLC44A2/HNA-3a group after LPS treatment suggests that SLC44A2 engagement induce neutrophil activation. NET formation is crucial during VT, and NETosis has been already described in TRALI after antibody binding to SLC44A2/HNA-3a and following a double “hit” scheme.

We chose to reproduce this model here, by stimulating neutrophils with LPS and by modulating a supplemental factor that could predispose to VT. During stasis, local concentrations in leukocytes can increase. We chose to perfuse different concentrations of LPS-pre-stimulated neutrophils through the VWF-coated flow chamber: equal concentration, concentration increased 5- or 10 times.

Two different brand of flow chambers were used, and fluorescence intensity visualization was set-up to allow focus on cell accumulation and not flowing cells. Cells were flowing as previously observed in the Ibidi chambers at “classic” concentration (Figure 4, upper left panel).

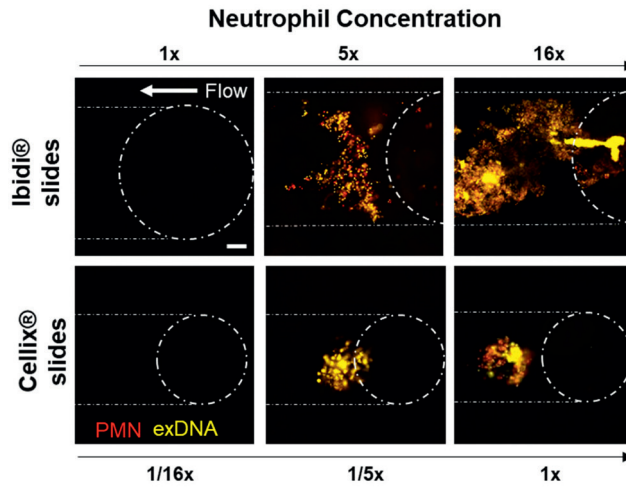


Figure 4. Neutrophils perfused on VWF can form DNA extracellular traps. Visualization of fluorescently-labeled neutrophils (PMN, red) and extracellular DNA (exDNA, yellow) after perfusion (100s^{-1} shear rate) on VWF of different concentrations of neutrophils (1x concentration= 1.5×10^6 cells/ml) in two different brands of flow chambers (n=2 donors, 3 fields per donor). Scale bar = $100\ \mu\text{m}$. Lines delimit the flow channels and the well entrance.

However, increasing cell concentration induced next to the entry of the chamber (where the rheological conditions are peculiar and where the cells are regaining speed) an accumulation of neutrophils (stained by calcein red orange) sticking together and to the chamber. The additional staining of extracellular DNA by the Sytox green dye suggests that these neutrophils could form NETs (Figure 4, upper middle and right panels) as shown by the presence of DNA fibers escaping from the adhering cells. This phenomenon was also observed when another chamber brand was used (Cellix slides), while ensuring that cell concentrations used are transposed to the rheological conditions and the geometry of the second chamber in order to be comparable (Figure 4, lower panels). We have found that this phenomenon could be amplified by increasing the intensity of the inflammatory stimulus from 5 to $25\ \mu\text{g/ml}$ LPS in the two different sets of flow chambers used (Figure S2 and Figure 5A). Interestingly the HNA-3b neutrophils did not react with the VWF matrix as HNA-3a neutrophils did, as they did not form extracellular DNA structures. This HNA-3a-dependent cell accumulation was calcium dependent, showing that extracellular DNA trap formation is an active phenomenon following the adhesion of neutrophils to the immobilized VWF under flow. We tested different matrices such as BSA, fibrinogen and VWF-A1 domain (Figure 5B) and confirmed to be in the presence of a VWF-A1-dependent phenomenon. *In vitro* incubation of TNF α primed-(mimicking LPS activation) HNA-3a-neutrophils with VWF resulted in an increase in the percentage of NET-forming cells (Figure 6) thus supporting the hypothesis that HNA-3a-bearing SLC44A2 can mediate neutrophil activation and NETosis in presence of VWF.

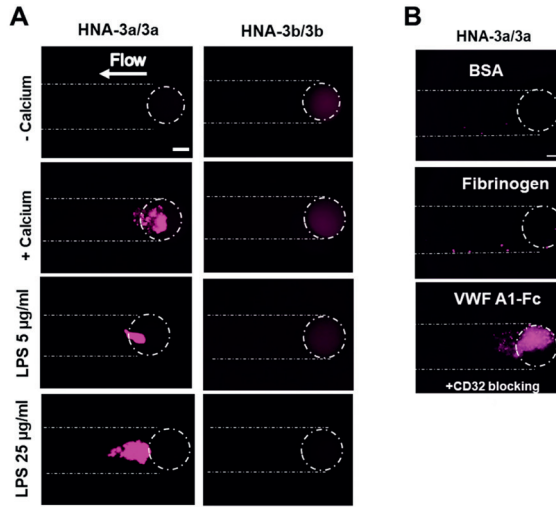


Figure 5. PMN activation on VWF at 100s⁻¹ is HNA-3a-, calcium-, VWF A1-domain-dependent, and can be exacerbated by LPS challenge. (A) Visualization of HNA-3a- or HNA-3b neutrophils (anti-Ly6G IgG) submitted to a 100s⁻¹ shear rate in absence or presence of calcium, or pre-activated with LPS prior to perfusion (5 or 25µg/ml) (Cellix brand flow chambers, n=3 donors per genotype). **(B)** Visualization of HNA-3a neutrophils perfused at a 100s⁻¹ shear rate on immobilized BSA, fibrinogen or VWF A1-Fc domain. Neutrophil Fc Receptors were blocked with anti CD32 antibody for A1 domain experiments. Scale bar=100 µm. Lines delimit the flow channels and the well entrance (n=3 donors per genotype).

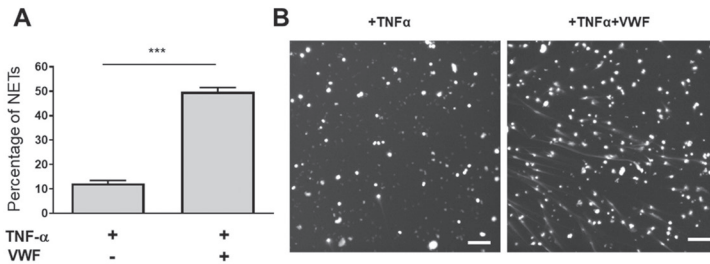


Figure 6. Primed neutrophils can form NETs under VWF challenge (A) Quantification of NETs after VWF challenge by fluorescence microscopy analysis. HNA-3a-positive neutrophils were primed with TNFα and incubated for 180 minutes with PBS (+TNFα) or VWF (+TNFα+VWF). DNA release was visualized after DNA staining with Hoescht 33342. The experiment was independently performed 2 times. **(B)** Example of the fluorescence images quantified in panel (A). Scale bar=100µm (*** p<0.005).

SLC44A2 play a major role in neutrophil recruitment at the vessel wall after endothelial degranulation in vivo

Through the use of human cells expressing either the HNA-3a or the HNA-3b epitope, we demonstrated an effect of SLC44A2 on neutrophil adhesion and activation on VWF under flow. In order to confirm our data *in vivo*, and because mice “knocked-in” for our polymorphism of interest do not exist yet, we used *Slc44a2* deficient mice and submitted them to the model of histamine-induced endothelial degranulation. Endothelial degranulation results in VWF release from the Weibel-Palade bodies. Mouse infusion with fluorescently labeled anti-Ly-6G antibody allowed us to track neutrophil accumulation at the vessel wall in this model. Our data confirmed our *in vitro* hypothesis: we observed a drastic reduction in neutrophil rolling and adhesion at the vessel wall of mesenteric venules (Figure 7, 409 ± 300 cells/min versus 59 ± 26 cells/min).

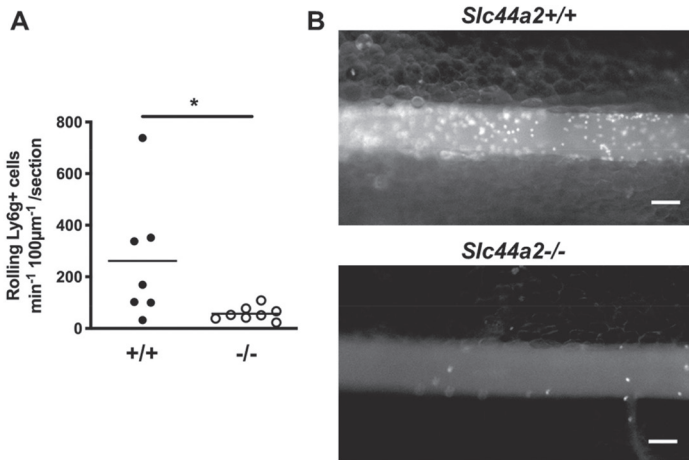


Figure 7. SLC44A2 is essential for neutrophil recruitment at the vessel wall following endothelial activation. Intravital microscopy was performed on mesenteric venules of SLC44A2 deficient mice (*Slc44a2*^{-/-}) and littermate wildtype controls (*Slc44a2*^{+/+}) after IP histamine challenge. **(A)** Quantification of neutrophil rolling on mesenteric venules in wildtype and SLC44A2 deficient mice (*Slc44a2*^{+/+}, n=7 venules in 3 mice; *Slc44a2*^{-/-}, n=8 venules in 3 mice). **(B)** Representative pictures showing reduced neutrophil recruitment in mesenteric venules of SLC44A2 deficient mice and wildtype after staining of endogenous rolling neutrophils by infusion of an Alexa 660-anti-Ly6g antibody. (* $p < 0.05$). Scale=100 μ m.

Discussion

In the present study, we demonstrated that SLC44A2 is involved in the adhesion and activation process of neutrophils on VWF and that this function is HNA 3a/HNA 3b

dependent. SLC44A2-mediated adhesion was VWF-A1 domain-dependent and enhanced under inflammatory stimulus, low shear rates (100s^{-1}) or specific rheologic conditions.

Recently, GWAS studies have homogeneously identified that *SLC44A2* was a new gene associated with the risk of VT. This was reinforced by mice data we and our collaborators obtained showing that absence of SLC44A2 is linked to reduced thrombus formation in the stenosis VT model (23). As pathophysiology of VT was mostly based on the original cascade model of coagulation and as *SLC44A2* does not belong to it, it is of major importance to characterize the biological link between this gene and VT. In the current study, we aimed to discover how the *SLC44A2* gene and the lead rs2288904 variant (461G>A; Arg154Gln) could affect SLC44A2 function in thrombosis.

This last decade, neutrophils and VWF have been shown to play a central role in VT. VWF is known to be an important protein in hemostasis by mediating platelet adhesion to the subendothelial matrix, but also in inflammation processes (for review (24)) that are crucial during VT development. SLC44A2 has been shown few years ago as a binding partner for VWF (10). However, how the Arg154Gln polymorphism could modulate this interaction had not been studied before. Because HNA-3b is associated with a decreased risk for VT over HNA-3a in patients (1, 2), we imagined a possible loss of function of SLC44A2 when exposing HNA-3b leading to a reduced binding of SLC44A2 to VWF.

We used HEK293T transfected cells, neutrophils and mice to assess the importance of SLC44A2 in the mechanisms of neutrophil adhesion to VWF *in vitro* and *in vivo*. We observed that the HNA-3a/HNA-3b epitope had no effect on neutrophil rolling when perfused on a VWF-coated matrix. However, SLC44A2/HNA-3a but not SLC44A2/HNA-3b allows cell adhesion to VWF when submitted to venous shear rates. Our *in vivo* data obtained in the mouse model of endothelial degranulation in mesenteric venules done on SLC44A2 deficient mice confirmed our hypothesis that SLC44A2 could be important for neutrophil recruitment at the vessel wall at venous shear rates and during inflammation.

Despite the fact that SLC44A2/HNA-3a-transfected HEK293T cells do not express beta 2 integrins (25), they adhere more on VWF than HEK293T cells expressing the HNA-3b form. This result suggests by itself that SLC44A2 can be sufficient to allow cell adhesion on VWF. However, subsequent integrin activation could potentialize SLC44A2-mediated adhesion of neutrophils as integrins have been described as playing a major role in leukocyte adhesion (26). The utilization of a β_2 -blocking antibody on neutrophils or the use of neutrophils purified from EDTA-anticoagulated blood (data not shown, chelation of divalent cations will not allow integrin activation) were not enough to abolish this neutrophil adhesion on VWF. Altogether these observations confirm that SLC44A2 is enough to induce cell adhesion on VWF under flow independently from integrins. However, our results and few hypotheses suggest that VWF/SLC44A2 interaction could also induce neutrophil and integrin activation thus consolidating the cell adhesion process. In TRALI for instance, anti-HNA-3a antibodies have

been shown to activate neutrophils (14). It is indeed possible that VWF has a comparable effect. Bayat and collaborators published evidence that following SLC44A2/VWF engagement VWF, SLC44A2, and Mac-1 ($\alpha_M\beta_2$) form a trimolecular complex at the neutrophil surface (10). This is a process expected to occur after “inside-out” signaling. An old study has also identified the SLC44A2-coding gene as able to activate the NF- κ B pathway (27). Interestingly, this pathway is essential for tissue factor expression in VT (28).

We have seen that a second hit can significantly affect SLC44A2-mediated neutrophil adhesion to VWF under flow. Inflammatory stimuli such as TNF- α or LPS, but also special rheologic conditions can in addition to HNA-3a expression stimulate NET formation. NETosis is an active process following neutrophil activation, crucial during VT (12, 18). NETs form a matrix for cell (platelets, red blood cells) or microparticle adhesion and form a thrombogenic surface exposing tissue factor or factor XII.

Our *in vivo* results obtained in the histamine-induced endothelial degranulation model support that SLC44A2 deficiency could delay both neutrophil recruitment and activation on a degranulated endothelium too. This may explain the phenotype of SLC44A2 deficient mice that formed smaller thrombi when submitted to the DVT stenosis model (23).

VWF and NETs are crucial in VT pathogenesis. It is also true for other pathologies linked to inflammation such as stroke or myocardial myocardial ischemia/reperfusion injury (29-32). HNA-3a has been found to be related to stroke too (1). Moreover stroke involves the VWF-A1 domain (33), which is the one important in SLC44A2-mediated adhesion as well. Our work thus suggests that GPIb may not be the only receptor involved when we talk about VWF-A1-associated thrombo-inflammatory pathogenesis. SLC44A2 has to be taken into consideration. VWF is released by endothelial cells through a constitutive pathway and through Weibel-Palade bodies release. VWF released from the storage compartment is of high molecular weight (34) and is released with a relatively high concentrations of calcium ions upon vascular injury or inflammatory stimulation. Our work suggests that SLC44A2 may be involved not only in VT but also in more pathologies than we originally thought in the inflammation field.

HNA-3b homozygous individuals being rare (6% of Caucasians)(21), it is easy to imagine that previous work on neutrophil adhesion and VWF used HNA-3a-positive donors for their work. In this study we point out the necessity to check on the HNA-3a/3b genotype of blood donors before purifying cells that will be used to work with VWF.

In conclusion, we propose here a new mechanism of neutrophil adhesion and activation that connects inflammation to thrombosis in veins. This mechanism involves the VWF-A1 domain and can induce neutrophil activation and NETosis. Other studies are thus warranted to better understand the mechanisms of SLC44A2/VWF molecular interaction and how this interaction can also influence neutrophil activation. Shutting down SLC44A2 function

would allow to target specifically thrombosis without affecting hemostasis, which would reduce the risk of hemorrhagic complications that are associated with actual prophylactic anticoagulant therapies.

Disclosure of Conflicts of Interest

The authors declare no competing financial interests.

Acknowledgments

The authors thank Thomas E. Carey (Kresge Hearing Research Institute, Department of Otolaryngology/Head and Neck Surgery, University of Michigan, Ann Arbor, MI, USA) for the floxed *Slc44a2* mouse embryos used to generate the mice on a C57BL/6j background; Matthias Canault and Cécile Denis for helpful discussions; and Brian Curtis, Daniel Bougie for providing us with the HEK293T transfected cells. This work was supported by the ANR (grant ANR-17-CE14-0003-01 to GMT).

Author contributions

Experimental design: GZ, JT, PR, CXM, PL, MCA, PJL, PEM, GMT. Performed experiments and analyzed data: GZ, JT, PR, CXM, PL, MCA, PJL, PEM, GMT. Wrote the paper: GZ, PR, PEM and GMT. All authors commented on manuscript drafts. All authors have approved the final version.

References

1. Hinds DA, Buil A, Ziemek D, et al. Genome-wide association analysis of self-reported events in 6135 individuals and 252 827 controls identifies 8 loci associated with thrombosis. *Human Molecular Genetics*. 2016;25(9):1867-74.
2. Germain M, Chasman DI, de Haan H, et al. Meta-analysis of 65,734 individuals identifies TSPAN15 and SLC44A2 as two susceptibility loci for venous thromboembolism. *Am J Hum Genet*. 2015;96(4):532-42.
3. Tilburg J, Coenen DM, Zirka G, et al. SLC44A2 deficient mice have a reduced response in stenosis but not in hypercoagulability driven venous thrombosis. *J Thromb Haemost*. 2020.
4. Kanack AJ, Peterson JA, Sullivan MJ, et al. Full-length recombinant choline transporter-like protein 2 containing arginine 154 reconstitutes the epitope recognized by HNA-3a antibodies. *Transfusion*. 2012;52(5):1112-6.
5. Greinacher A, Wesche J, Hammer E, et al. Characterization of the human neutrophil alloantigen-3a. *Nature Medicine*. 2010;16(1):45-8.
6. Curtis BR, Sullivan MJ, Holyst MT, et al. HNA-3a-specific antibodies recognize choline transporter-like protein-2 peptides containing arginine, but not glutamine at Position 154. *Transfusion*. 2011;51(10):2168-74.
7. Flesch BK, Wesche J, Berthold T, et al. Expression of the CTL2 transcript variants in human peripheral blood cells and human tissues. 2013;53(12):3217-23.
8. Traiffort E, O'Regan S, Ruat M. The choline transporter-like family SLC44: properties and roles in human diseases. *Mol Aspects Med*. 2013;34(2-3):646-54.
9. Kommareddi PK, Nair TS, Thang LV, et al. Isoforms, Expression, Glycosylation, and Tissue Distribution of CTL2/SLC44A2. *The Protein Journal*. 2010;29(6):417-26.
10. Bayat B, Tjahjono Y, Berghofer H, et al. Choline Transporter-Like Protein-2: New von Willebrand Factor-Binding Partner Involved in Antibody-Mediated Neutrophil Activation and Transfusion-Related Acute Lung Injury. *Arterioscler Thromb Vasc Biol*. 2015;35(7):1616-22.
11. Brill A, Fuchs TA, Savchenko AS, et al. Neutrophil extracellular traps promote deep vein thrombosis in mice. 2012;10(1):136-44.
12. Martinod K, Demers M, Fuchs TA, et al. Neutrophil histone modification by peptidylarginine deiminase 4 is critical for deep vein thrombosis in mice. *Proc Natl Acad Sci U S A*. 2013;110(21):8674-9.
13. Brill A, Fuchs TA, Chauhan AK, et al. von Willebrand factor-mediated platelet adhesion is critical for deep vein thrombosis in mouse models. *Blood*. 2011;117(4):1400-7.
14. Thomas GM, Carbo C, Curtis BR, et al. Extracellular DNA traps are associated with the pathogenesis of TRALI in humans and mice. *Blood*. 2012;119(26):6335-43.
15. Berthold T, Muschter S, Schubert N, et al. Impact of priming on the response of neutrophils to human neutrophil alloantigen-3a antibodies. *Transfusion*. 2015;55(6 Pt 2):1512-21.
16. Caudrillier A, Kessenbrock K, Gilliss BM, et al. Platelets induce neutrophil extracellular traps in transfusion-related acute lung injury. *J Clin Invest*. 2012;122(7):2661-71.
17. Darbousset R, Thomas GM, Mezouar S, et al. Tissue factor-positive neutrophils bind to injured endothelial wall and initiate thrombus formation. *Blood*. 2012;120(10):2133-43.

18. von Bruhl ML, Stark K, Steinhart A, et al. Monocytes, neutrophils, and platelets cooperate to initiate and propagate venous thrombosis in mice in vivo. *J Exp Med*. 2012;209(4):819-35.
19. Fuchs TA, Brill A, Wagner DD. Neutrophil extracellular trap (NET) impact on deep vein thrombosis. *Arterioscler Thromb Vasc Biol*. 2012;32(8):1777-83.
20. Bougie DW, Peterson JA, Kanack AJ, et al. Transfusion-related acute lung injury-associated HNA-3a antibodies recognize complex determinants on choline transporter-like protein 2. *Transfusion*. 2014;54(12):3208-15.
21. Bowens KL, Sullivan MJ, Curtis BR. Determination of neutrophil antigen HNA-3a and HNA-3b genotype frequencies in six racial groups by high-throughput 5' exonuclease assay. *Transfusion*. 2012;52(11):2368-74.
22. Wang P, Wu P, Anthes JC, et al. Interleukin-10 inhibits interleukin-8 production in human neutrophils. *Blood*. 1994;83(9):2678-83.
23. Tilburg J, Michaud SA, Maracle CX, et al. Plasma Protein Signatures of a Murine Venous Thrombosis Model and Slc44a2 Knockout Mice Using Quantitative-Targeted Proteomics. *Thromb Haemost*. 2020;120(3):423-36.
24. Kawecki C, Lenting PJ, Denis CV. von Willebrand factor and inflammation. *J Thromb Haemost*. 2017;15(7):1285-94.
25. Gupta V, Alonso JL, Sugimori T, et al. Role of the beta-subunit arginine/lysine finger in integrin heterodimer formation and function. *J Immunol*. 2008;180(3):1713-8.
26. Kuijpers TW, Van Lier RA, Hamann D, et al. Leukocyte adhesion deficiency type 1 (LAD-1)/variant. A novel immunodeficiency syndrome characterized by dysfunctional beta2 integrins. *J Clin Invest*. 1997;100(7):1725-33.
27. Matsuda A, Suzuki Y, Honda G, et al. Large-scale identification and characterization of human genes that activate NF-kappaB and MAPK signaling pathways. *Oncogene*. 2003;22(21):3307-18.
28. Li YD, Ye BQ, Zheng SX, et al. NF-kappaB transcription factor p50 critically regulates tissue factor in deep vein thrombosis. *J Biol Chem*. 2009;284(7):4473-83.
29. Zhao BQ, Chauhan AK, Canault M, et al. von Willebrand factor-cleaving protease ADAMTS13 reduces ischemic brain injury in experimental stroke. *Blood*. 2009;114(15):3329-34.
30. Hillgruber C, Steingraber AK, Poppelmann B, et al. Blocking von Willebrand factor for treatment of cutaneous inflammation. *J Invest Dermatol*. 2014;134(1):77-86.
31. Savchenko AS, Martinod K, Seidman MA, et al. Neutrophil extracellular traps form predominantly during the organizing stage of human venous thromboembolism development. *J Thromb Haemost*. 2014;12(6):860-70.
32. Dhanesha N, Prakash P, Doddapattar P, et al. Endothelial Cell-Derived von Willebrand Factor Is the Major Determinant That Mediates von Willebrand Factor-Dependent Acute Ischemic Stroke by Promoting Postischemic Thrombo-Inflammation. *Arterioscler Thromb Vasc Biol*. 2016;36(9):1829-37.
33. Denorme F, Martinod K, Vandenbulcke A, et al. The von Willebrand Factor A1 domain mediates thromboinflammation, aggravating ischemic stroke outcome in mice. *Haematologica*. 2020.
34. Wagner DD. Cell biology of von Willebrand factor. *Annu Rev Cell Biol*. 1990;6:217-46.

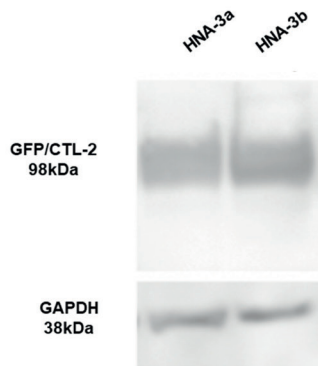


Figure S1. Western blot of transfected HNA-3a- and HNA-3b-expressing HEK293T cell lysates probed with an antibody directed against GFP or GAPDH.

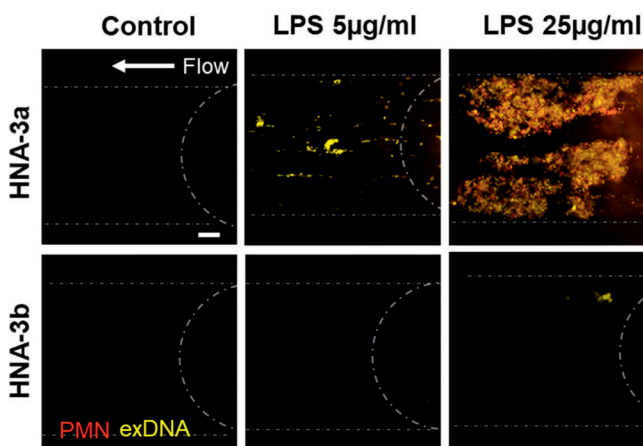


Figure S2. Visualization of fluorescently-labeled HNA-3a- or HNA-3b- neutrophils (PMN, red) stimulated with LPS (5 or 25µg/ml) and extracellular DNA (exDNA, yellow) after perfusion (100s^{-1} shear rate) on VWF-coated flow chambers. (n=3 donors per genotype). Scale bar =100 µm. Lines delimit the flow channels and the well entrance.

